

Valence compensation of thermally generated $[\text{Li}]^0$ defects in MgO

J. L. Boldu,* M. M. Abraham, and Y. Chen

Solid State Division, Oak Ridge National Laboratory

Oak Ridge, Tennessee 37830

(Received 19 December 1978)

The creation of thermally generated $[\text{Li}]^0$ defects (configuration: $\text{O}^{2-} - \text{Li}^+ - \text{O}^-$) and other lithium-associated centers in MgO is attended by valence changes of transition-metal impurities, such as Fe and Cr. The electron-paramagnetic-resonance (EPR) technique was used to monitor the concentrations of these impurities and the $[\text{Li}]^0$ defects as a function of the incubating temperature in static air. Although near the threshold temperature for $[\text{Li}]^0$ production the impurities may contribute a significant portion of the holes needed for the valence compensation of stable $[\text{Li}]^0$ defects, at higher temperatures (~ 1600 K) they can supply only a small percentage of the holes required. Since oxygen was found to be necessary for the formation of $[\text{Li}]^0$ defects, the primary source of holes at these high temperatures is attributed to the surface reaction: $\text{O}_2 \rightarrow 2\text{O}^{2-} + 4$ holes. The effects of optical bleaching and ionizing radiation at 77 K on the concentrations were studied as a function of incubating temperatures. Electron-nuclear double resonance (ENDOR) was used to probe the local environments of the $[\text{Li}]^0$ defects and other lithium-associated centers.

I. INTRODUCTION

Lithium-doped MgO crystals, when exposed to elevated temperatures, exhibit a deep blue coloration which has been attributed to the optical-absorption band of the $[\text{Li}]^0$ defect (linear configuration: $\text{Mg}^{2+} - \text{O}^{2-} - \text{Li}^+ - \text{O}^- - \text{Mg}^{2+}$).^{1,2} These $[\text{Li}]^0$ defects are unusual in that they are much more stable against hole release than their counterparts produced by ionizing radiation³⁻⁷ at low temperatures. Previous work has established the presence of Li_2O precipitates⁸ in the MgO matrix which diminish in size upon exposure to high temperatures in air. The Li^+ ions which disperse from the precipitates form a lithium-rich environment (microgalaxy)² containing stable $[\text{Li}]^0$ defects. Stable $[\text{Li}]^0$ defects can be thermally generated only when the crystal is heated in an atmosphere containing oxygen⁹; that is, these defects cannot be produced in inert or reducing atmospheres.

MgO crystals, including the nominally pure ones, normally contain Fe, Cr, and Mn as unavoidable impurities.¹⁰ These impurities play an important role in the charge compensation of intrinsic and extrinsic defects in the crystals. Indeed, in the case of $[\text{Li}]^0$ defect generated by low-temperature irradiations, the compensation of the hole is attended by the trapping of an electron at impurity sites, such as iron, reducing Fe^{3+} to Fe^{2+} . The formation of stable $[\text{Li}]^0$ defects is an important part of the mechanism for lithium transport in MgO. In this respect, it is essential to understand the role of impurities in the $[\text{Li}]^0$ for-

mation and how these impurities respond to various environments. The purposes of this study were (i) to investigate lithium-associated centers and to probe for possible local environmental differences between stable and unstable $[\text{Li}]^0$ defects, (ii) to study quantitatively the charge compensation of the $[\text{Li}]^0$ defects and other paramagnetic impurities in the crystal, and (iii) to explore this charge compensation following ionizing irradiation and light excitation.

II. EXPERIMENTAL PROCEDURE

Single crystals were grown by the arc fusion method¹⁰ employing a mixture of 5% Li_2CO_3 by weight in MgO powder obtained from the Kanto Chemical Company (Tokyo). The actual concentration of lithium in the resulting single crystals was determined by spectrographic analyses to be approximately 0.03 - 0.05 at.%.¹¹ A Sentry Model 7AV furnace with a quartz tube inserted in the horizontal axial hole was used for heating the samples. The samples were heated in static air (no air flowing) for 7 min and pulled out to be cooled in the room-temperature portion of the quartz tube.

After each thermal quenching, an EPR spectrum (X band) was measured at 87 ± 1 K in a Varian 4531 cavity. After a 10-min bleaching with a He-Ne laser (632.8 nm) *in situ*, another spectrum was taken. The crystal was then removed to be irradiated in a ^{137}Cs γ source at 77 K. Without an intervening warmup, the

sample was placed again in the cavity and another EPR spectrum was obtained. These procedures were then repeated for the next quenching temperature.

The absolute concentrations of the various defects in the samples were determined by comparing the resonance line of the defects to that of the Cr^{3+} signal from an MgO single crystal. The Cr^{3+} concentration of this sample was standardized by several techniques.¹² The values of the absolute concentrations reported in this paper are believed to be accurate within $\pm 25\%$.

III. RESULTS AND DISCUSSION

A. $[\text{Li}]^0$ and other impurities

Figure 1 shows a plot of the absolute concentrations as determined by EPR, of all the dominant paramagnetic impurities versus the quenching temperature. It can be seen that no drastic concentration change occurs below $T \sim 1200$ K. This value approximated the threshold temperature for the thermal generation of stable $[\text{Li}]^0$ defects in static air, as pre-

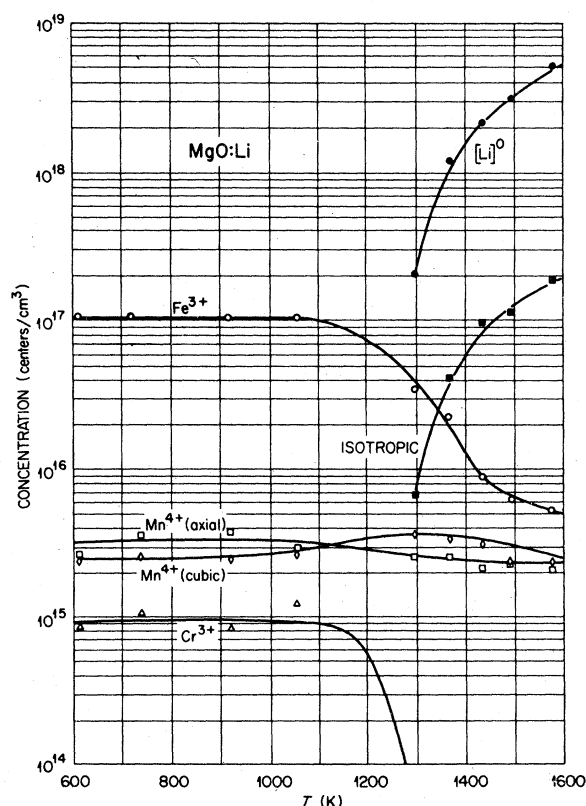


FIG. 1. Absolute concentrations of paramagnetic impurities in MgO:Li as a function of the quenching temperature.

viously determined by optical-absorption measurements.² A sizable concentration of $[\text{Li}]^0$ defects ($2 \times 10^{17} \text{ cm}^{-3}$) was generated at 1300 K and continued to increase at least up to $T \sim 1600$ K. With the emergence of the $[\text{Li}]^0$ signal, an isotropic signal ($g = 2.014 \pm 0.001$) appeared¹ and also grew in intensity with increasing incubating temperature. Since this signal has been observed only in lithium-doped crystals, it is attributed to a lithium-associated defect. The trivalent impurities Fe^{3+} and Cr^{3+} , on the other hand, diminished in intensity with increasing incubating temperature, suggesting that they contribute to the charge compensation of the $[\text{Li}]^0$ and the isotropic defects. Both the axial and cubic Mn^{4+} concentrations do not appear to be strongly affected by the $[\text{Li}]^0$ formation.

Since iron and lithium represent the most abundant impurities identified in the crystal, we can compare the increase of the $[\text{Li}]^0$ concentration to the decrease of Fe^{3+} . (From Fig. 1, it is clear that Cr and Mn are at least two orders of magnitude less abundant.) In Fig. 2, a plot of the concentration ratio of the thermally generated $[\text{Li}]^0$ to the loss of Fe^{3+} versus the incubating temperature is shown. In effect, this figure describes the fractional contribution of holes from the Fe^{3+} to the $[\text{Li}]^0$ defects. The ratio increased with temperature and was > 60 at $T \sim 1600$ K. However, this ratio was sample dependent and ranged from 40–100 at $T \sim 1600$ K depending on the total iron and lithium concentrations present.

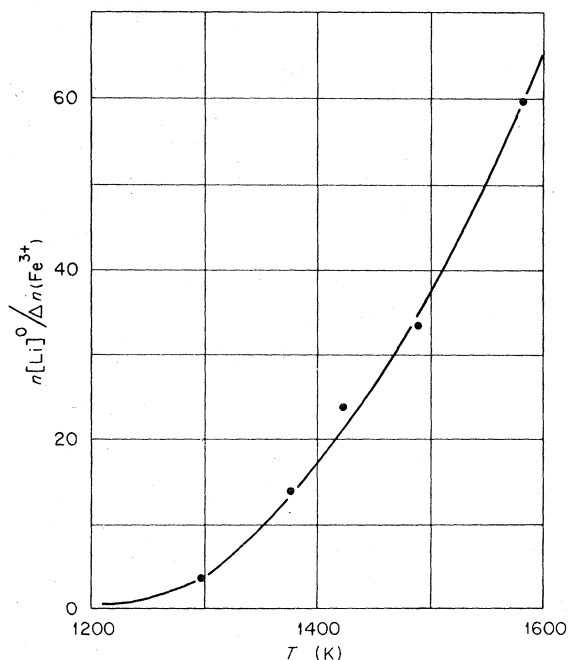


FIG. 2. Concentration ratio of $[\text{Li}]^0$ to Fe^{3+} as a function of quenching temperature.

This indicated that impurities are not sufficient to charge compensate for the thermal generation of $[\text{Li}]^0$ defects, especially at very high temperatures.

B. Effects of optical bleaching and γ irradiation

Optical bleaching and ionizing irradiation were performed at 77 K after each thermal treatment. The 632.8-nm (1.96 eV) wavelength of the laser is sufficiently close to the 1.83 eV peak of the broad $[\text{Li}]^0$ absorption band that it can be considered as bleaching into the optical band. The effect of the bleaching and γ irradiation on the cubic Fe^{3+} concentration is shown in Fig. 3. Below the threshold temperature for $[\text{Li}]^0$ formation, the Fe^{3+} signal intensity was not affected by the bleaching whereas at higher temperatures, its concentration increased. The subsequent γ irradiation tends to restore the initial Fe^{3+} concentration. Therefore it would appear that the restoration of cubic Fe^{3+} was due to conversions from cubic Fe^{2+} and/or Fe^+ by the capture of holes. However, our EPR experiments (both *X*- and *K*-band microwave frequencies) at 4.2 K showed no evidence for cubic Fe^{2+} or Fe^+ in any of these lithium-doped samples, either before or after heat treatments. It is possible, although not likely, that the signals of these two species were too small to be detected. As a check to determine instrumental sensitivity, we had no

difficulty in observing (at *K* band) the $\Delta M_s = \pm 1, \Delta M_s = \pm 2$, and the double-quantum transitions ($g \sim 3.43$ and 6.83) of Fe^{2+} in cubic symmetry¹³ for nominally pure or Fe-doped MgO; in these crystals the isotropic Fe^+ signal¹⁴ at $g \sim 4.13$ was also easily obtained at *X* band following irradiation at low temperature. Another possibility for the Li-doped samples is that the bleaching-and ionization-induced cubic Fe^{3+} ions were formed at the expense of sites whose symmetry is lower than cubic. Presumably these monovalent and divalent Fe ions would thereby escape EPR detection. However, since the bleaching and γ irradiation were performed near 80 K, it is difficult to visualize that ionic mobility can occur at that temperature, and change the local symmetry around Fe ions.

Figure 4 illustrates the thermal dependence of the $[\text{Li}]^0$ concentration upon laser bleaching and γ irradiation. For this sample, laser bleaching had a more pronounced effect on the $[\text{Li}]^0$ concentration below 1400 K that at higher incubating temperatures. Ionizing radiation further increased the $[\text{Li}]^0$ concentration. These increases are due to the creation of unstable $[\text{Li}]^0$ defects. Upon warming the crystal to room temperature the $[\text{Li}]^0$ concentration indeed reverted back to the prebleaching level.

In this connection, it is appropriate to remark on our ENDOR observations on stable and unstable $[\text{Li}]^0$ defects. Both the $[\text{Li}]^0$ line positions^{1,5} and

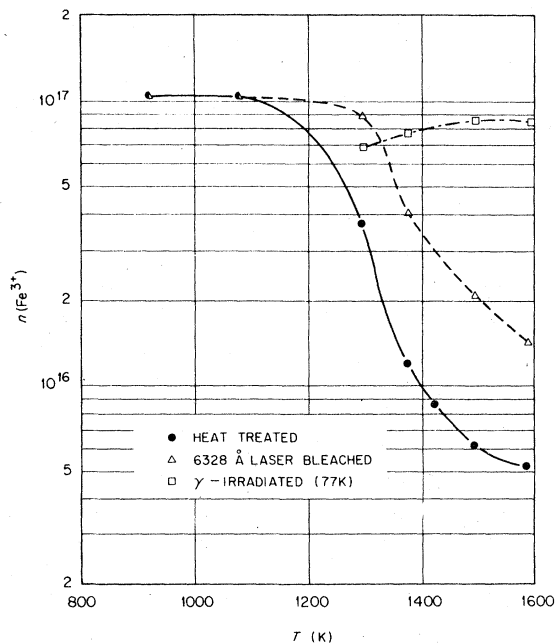


FIG. 3. Absolute concentration (centers/cm³) of Fe^{3+} in cubic sites as a function of quenching temperature. Broken curves represent concentrations after the corresponding additional treatments.

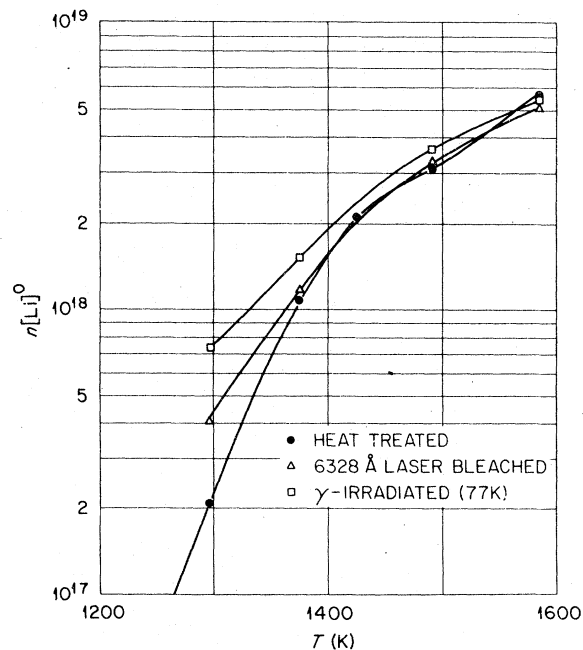


FIG. 4. Absolute concentration (centers/cm³) of stable $[\text{Li}]^0$ defects as a function of quenching temperature.

linewidths are the same for γ -irradiated and quenched crystals. This indicates that there is no difference in configuration between the stable and unstable $[\text{Li}]^0$ defects. Even when the $[\text{Li}]^0$ concentrations were vastly different, no difference in ENDOR linewidths were observed. However, a large ENDOR linewidth variation as a function of the nuclear rf power was found for both species. A 10-kHz linewidth was observed for an applied power of 0.5 watts or less, while a maximum value of 20 kHz was obtained at 5 or more watts. This rf power broadening was accompanied by extra signals, implying hole hopping for powers above a few watts. Above 5 watts, double quantum transitions could be observed.

In contrast to the $[\text{Li}]^0$ defect, the isotropic signal diminished in intensity after the laser bleaching (Fig. 5). The subsequent γ irradiation increased the signal intensity at 1300 K, but above 1400 K the signal was undetectable. Since this defect has not been identified, its contribution to the charge-balance mechanism can not be assessed. From the present results, it is not possible to unequivocally deduce whether the defect is a hole or an electron trapping defect.

C. Aggregates

Figure 6 displays the spectra of two different defects which were created under different circumstances but which appeared in the same magnetic field region. Figure 6(b) shows the previously observed spectrum¹ found in a thermally treated crystal and tentatively assigned to "lithium pairs." Although there is an axial Mn^{4+} hyperfine set¹⁵ overlapping the seven hyperfine lines, it is easy to see that they closely follow a proper 1:2:3:4:3:2:1 intensity distribution

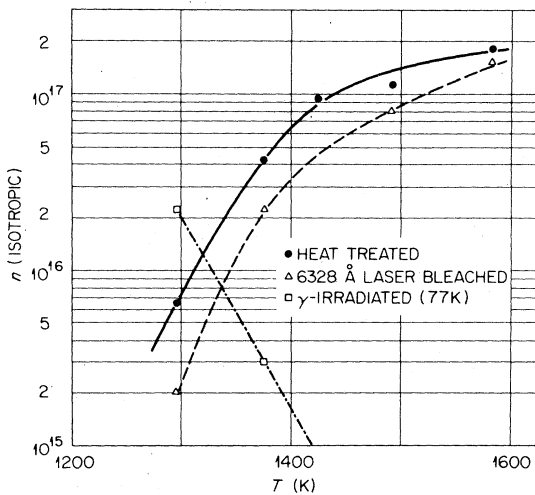


FIG. 5. Absolute concentration (centers/cm³) of the isotropic center as a function of quenching temperature.

with a hyperfine coupling constant of ~ 2.0 G. Figure 6(a) shows exactly the same portion of the spectrum for an "as-grown" sample that has been γ irradiated at 77 K. The structure is different and appears to be formed by three different sets of seven hyperfine lines, each with an approximate average spacing of 2.5 G. In this case, the axial Mn^{4+} hyperfine lines have reached a minimum intensity value due to the radiation-induced conversion of Mn^{4+} into Mn^{2+} . Clearly this is indicative of aggregates involving multiple lithium ions. In both cases, angular variation measurements could not be made, due to the multiplicity of the lines when the magnetic field was not parallel to the $\langle 100 \rangle$ axis. Several attempts were made to find lithium ENDOR signals with $\vec{H} \parallel \langle 100 \rangle$ for both types of aggregates, but none of them was successful. Moreover, an exhaustive ENDOR search for any other associated nuclei was also unfruitful.

The thermal stability of these two types of lithium aggregates is different. The lithium pair spectrum in the quenched samples is stable indefinitely at room temperature. However, the radiation-induced signals are unstable, even though they decay at a much

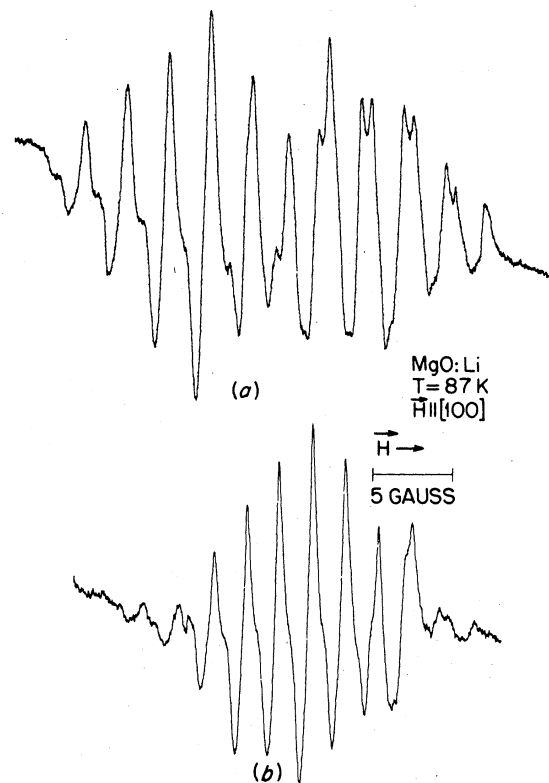


FIG. 6. EPR spectra of lithium aggregates: (a) samples γ irradiated at 77 K and (b) same sample quenched from 1300 K.

slower rate than the unstable $[\text{Li}]^0$ defects. This is illustrated in Fig. 7 where the spectral changes for the γ -induced lithium aggregate set [Fig. 7(a)] are shown along with the spectral change observed after a subsequent 2-min thermal anneal at 233 K [Fig. 7(b)] and at 243 K [Fig. 7(c)]. It can also be observed that Mn^{4+} signals reappeared as the aggregate signals decreased in intensity.

The production of the thermally generated "lithium pairs" as a function of incubating temperature is different from that of the $[\text{Li}]^0$ defects. Whereas the maximum $[\text{Li}]^0$ concentration in this study occurs at 1600 K, the pair signals showed their maximum intensity when the quenching temperature was near the threshold point for $[\text{Li}]^0$ production. The pair signals decreased in intensity with rising incubating temperature and disappeared as T approached 1600 K.

It should be noted that, following the low-temperature γ irradiation two groups of lines approximately 450 G apart are present in the EPR spectrum: one group near the $m_l = +\frac{5}{2}$ cubic Mn^{2+} line and the other group near the $m_l = -\frac{5}{2}$ cubic Mn^{2+} line. With the magnetic field along the [100] direction, each group appears to be a single set of four hyperfine lines with an approximate 9 G separation between them. Upon rotation of the magnetic field, the larger separation remains roughly isotropic, and each set of four lines splits into eight lines; i.e., the [100] direc-

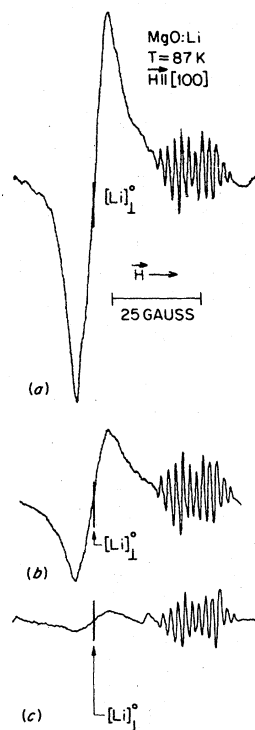


FIG. 7. EPR spectra of $\text{MgO}:\text{Li}$ crystal (a) γ irradiated at 77 K and subsequent two-minute thermal anneals at (b) 233 K and (c) 243 K.

tion represents a coalescence of lines from at least two different sites. Due to their low intensity, the angular variation of these lines was difficult to follow, and they had longer relaxation times than either the Mn^{2+} and $[\text{Li}]^0$ signals, making their observation difficult at high microwave powers. These lines have been observed in MgO only when it contains lithium as an impurity, and their pattern is similar to that previously observed in lithium-doped CaO and proposed to be due to a lithium-hydrogen complex.¹⁶ Unfortunately, since the conditions were not favorable for an ENDOR investigation, these centers could not be uniquely identified.

IV. CONCLUSION

It is clear that the total amount of all the paramagnetic impurities cannot be equated with the number of stable $[\text{Li}]^0$ defects formed. Fe^{3+} is the predominant paramagnetic impurity in our crystals, as illustrated in Fig. 1. Figure 2 shows that, at 1300 K, the iron can contribute a significant fraction of the holes for the valence compensation of stable $[\text{Li}]^0$ defects. However, at 1600 K, Fe^{3+} is clearly inadequate, since it can supply only 1–2% of the holes required. (A diamagnetic impurity contributing a hole would likely become paramagnetic and therefore detectable. The unknown isotropic signal may be due to such a defect.) Furthermore, at this temperature, any impurity valence changes induced by the bleaching and ionizing irradiation do not change the concentration of $[\text{Li}]^0$ centers by more than $5 \times 10^{17} \text{ cm}^{-3}$ (Fig. 4).

Our present understanding is that at elevated temperatures, the monovalent lithium ions abandon the Li_2O precipitates and replace magnesium sites around the precipitates, provided the sample is immersed in an atmosphere containing oxygen. Each of these substitutional Li^+ ions serve to capture a hole and can be identified as a neutral $[\text{Li}]^0$ defect. The dissociation of molecular oxygen at the surface into oxygen ions provides the required source of positive holes. This process is represented by



The presence of holes at the $[\text{Li}]^0$ sites is a necessary condition for Li^+ ions to leave Li_2O precipitates and occupy magnesium sites in a microgalaxy. Without these holes, such a region (microgalaxy) would not have been formed in the first place, since the Li^+ ions cannot remain in substitutional positions without charge compensation. Without oxygen, the ions which have dissolved in the matrix at high temperature, must at low temperature either return to the Li_2O precipitates or aggregate into a new form, such as a metallic precipitate. Accordingly, there will be no stable $[\text{Li}]^0$ defects formed, as in fact observed in crystals quenched in inert or reducing atmospheres. Therefore, the presence of oxygen serves to satisfy

both ionic and electronic requirements for the formation of stable $[\text{Li}]^0$ defects. The net reaction is



where (Li^+O^-) is the $[\text{Li}]^0$ defect.

ACKNOWLEDGEMENT

This Research was sponsored by the Division of Materials Sciences, U.S. DOE under Contract No. W-7405-eng-26 with the Union Carbide Corporation.

*Permanent address: Instituto de Fisica, U. N. A. M. Mexico, D. F.

¹M. M. Abraham, Y. Chen, L. A. Boatner, and R. W. Reynolds, *Phys. Rev. Lett.* **37**, 849 (1976).

²Y. Chen, H. T. Tohver, J. Narayan, and M. M. Abraham, *Phys. Rev. B* **16**, 5535 (1977).

³G. Rius, R. Cox, R. Picard, and C. Santier, *C. R. Acad. Sci.* **271**, 724 (1970).

⁴O. F. Schirmer, *J. Phys. Chem. Solids* **32**, 499 (1971).

⁵M. M. Abraham, W. P. Unruh, and Y. Chen, *Phys. Rev. B* **10**, 3540 (1974).

⁶G. Rius and A. Herve, *Solid State Comm.* **15**, 399 (1974); **15**, 421 (1974).

⁷G. Rius, A. Herve, R. Picard, and C. Santier, *J. Phys. (Paris)* **37**, 129 (1976).

⁸J. Narayan, M. M. Abraham, Y. Chen, and H. T. Tohver, *Philos. Mag. A* **37**, 909 (1978).

⁹J. B. Lacy, M. M. Abraham, J. L. Boldu O., Y. Chen, J. Narayan, and H. T. Tohver, *Phys. Rev. B* **19**, (1978).

¹⁰M. M. Abraham, C. T. Butler, and Y. Chen, *J. Chem. Phys.* **55**, 3757 (1971).

¹¹Y. Chen and M. M. Abraham, *J. Am. Ceram. Soc.* **59**, 101 (1976).

¹²Y. Chen, M. M. Abraham, L. C. Templeton, and W. P. Unruh, *Phys. Rev. B* **11**, 881 (1975).

¹³W. Low, in *Paramagnetic Resonance in Solids, Solid State Physics*, edited by F. Seitz and D. Turnbull, (Academic, New York, 1960), Suppl. 2, p. 85.

¹⁴J. W. Orton, P. Auzins, J. H. E. Griffiths, and J. E. Wertz, *Proc. Phys. Soc. London* **78**, 554 (1961).

¹⁵J. Rubio O., Y. Chen, and M. M. Abraham, *J. Chem. Phys.* **64**, 4804 (1976).

¹⁶B. Henderson and H. T. Tohver, *Phys. Status Solidi B* **51**, 761 (1972).